© 2019. Published by The Company of Biologists Ltd | Development (2019) 146, dev172866. doi:10.1242/dev.172866

RESEARCH ARTICLE

The central nervous system acts as a transducer of stress-induced masculinization through corticotropin-releasing hormone B

Diana C. Castañeda Cortés[1], Luisa F. Arias Padilla[1], Valérie S. Langlois[2], Gustavo M. Somoza[3] and Juan I. Fernandino[1,*]

ABSTRACT

Exposure to environmental stressors, such as high temperature (HT), during early development of fish induces sex reversal of genotypic females. Nevertheless, the involvement of the brain in this process is not well clarified. In the present work, we investigated the mRNA levels of corticotropin-releasing hormone b (*crhb*) and its receptors (*crhr1* and *crhr2*), and found that they were upregulated at HT during the crucial period of gonadal sex determination in medaka. In order to clarify their roles in sex reversal, biallelic mutants for *crhr1* and *crhr2* were produced by CRISPR/Cas9 technology. Remarkably, biallelic mutants of both loci (*crhr1* and *crhr2*) did not undergo female-to-male sex reversal upon exposure to HT. Inhibition of this process in double corticotropin-releasing hormone receptor mutants could be successfully rescued through the administration of the downstream effector of the hypothalamic-pituitary-interrenal axis, cortisol. Taken together, these results reveal for the first time that the CNS acts as a transducer of masculinization induced by thermal stress.

KEY WORDS: Environmental stress, CRH, Masculinization, CRISPR/Cas9, Medaka

INTRODUCTION

As a general trend, the response of the neuroendocrine system to environmental stressors is elevation of hypothalamic corticotropin-releasing hormone (Crh). Crh in turn stimulates the secretion and release of adrenocorticotropic hormone (Acth) from the pituitary gland (Aguilera and Liu, 2012; Kovács, 2013), which regulates cortisol levels through the adrenal gland (Mommsen et al., 1999). This is known as the hypothalamic-pituitary-adrenal (HPA) axis or the hypothalamic-pituitary-interrenal (HPI) axis in tetrapods and fish, respectively. In the latter, two *crh* ohnologs, named *crha* and *crhb*, have been identified (Grone and Maruska, 2015). The expression of *crha* has been mainly observed in the retina (Grone and Maruska, 2015; Hosono et al., 2015), with weak expression in the brain (about 100 times less than in retina) (Hosono et al., 2015), in fish. By contrast, *crhb* is mainly expressed in the central nervous system (CNS), i.e. in the preoptic area, the hypothalamus and the caudal neurosecretory system. For this reason, it has been related to the control of Acth in the pituitary gland (Alderman and Bernier, 2009; Bernier et al., 2008; Carpenter et al., 2014; Chen and Fernald, 2008; Grone and Maruska, 2015).

The action of Crh in the pituitary is mediated by the binding and activation of two highly conserved membrane receptors (Crhr1 and Crhr2), which belong to class B of the G protein-coupled receptors (Lovejoy et al., 2014). Although in tetrapods, it has been reported that Crh has higher affinity for Crhr1 (Vaughan et al., 1995), in teleosts both Crh ligands have similar affinity for both Crh receptors (Hosono et al., 2015). Several studies in mammals have also demonstrated the ability of Crh receptor antagonists to block stress responses, such as anxiety or depression (Backström and Winberg, 2013; Grammatopoulos and Chrousos, 2002; Holsboer and Ising, 2008), placing Crh receptors at a crucial point in regulation of the HPA axis.

The molecular and morphological processes of masculinization by stress have been investigated at the local, gonadal level, in several species from nematodes (Chandler et al., 2012, 2008), fish (Hattori et al., 2007; Hayashi et al., 2010; Kitano et al., 2012) and amphibians (Nakamura, 2009), to reptiles (Ge et al., 2018; Mork et al., 2014; Yatsu et al., 2015), but the involvement of the brain in sex-reversal is still under scrutiny. In all these vertebrates, exposure to environmental stressors during early life has several implications in reproduction. For instance, when reptiles and fish are exposed to stress during the crucial period of gonadal differentiation, a strong bias in sex ratios can be induced (Capel, 2017; Fernandino et al., 2013). The downstream factors involved in stress-induced masculinization in fish are well known (Hattori et al., 2009; Hayashi et al., 2010; Mankiewicz et al., 2013; Ribas et al., 2017; Tsalafouta et al., 2014; Yamaguchi et al., 2010). These factors can act by three different mechanisms: (1) inhibition of estrogen synthesis (Kitano et al., 2012; Nozu and Nakamura, 2015), (2) elevation of androgen synthesis (Fernandino et al., 2012; Hattori et al., 2009), and (3) apoptosis or meiotic arrest of germ cells (Yamaguchi and Kitano, 2012; Yamamoto et al., 2013). However, the molecular processes and key players controlling cortisol increase, which regulates these three mechanisms, remain unexplored.

In this study, we provide clear evidence of the role of the CNS in regulation of the HPI axis, shedding light on the triggering mechanism of masculinization induced by environmental factors.

RESULTS

Expression of corticotropin-related genes reared at high temperature

First, we examined the regulation of both *crh* paralogs under normal and masculinizing temperature. The mRNA levels of *crha* and *crhb* were analyzed in medaka embryos at stages 26, 33 and 37, incubated at control (24°C; CT) or high (32°C; HT) temperatures (Fig. 1). No differences were detected for *crha* between treatments, at any of the developmental stages examined (Fig. 1A). In contrast, we observed high transcript levels of *crhb* under HT conditions at stage 37, corresponding to the gonadal sex

[1]Laboratorio de Biología del Desarrollo - Instituto Tecnológico de Chascomús, INTECH (CONICET-UNSAM), Chascomús B7130IWA, Argentina. [2]Institut National de la Recherche Scientifique (INRS) - Centre Eau Terre Environnement, Quebec G1K 9A9, Canada. [3]Laboratorio de Ictiofisiología y Acuicultura - INTECH (CONICET-UNSAM), Chascomús B7130IWA, Argentina.

*Author for correspondence (fernandino@intech.gov.ar)

J.I.F., 0000-0003-1754-2802

Received 15 October 2018; Accepted 21 March 2019

Development (2019) 146, dev172866. doi:10.1242/dev.172866

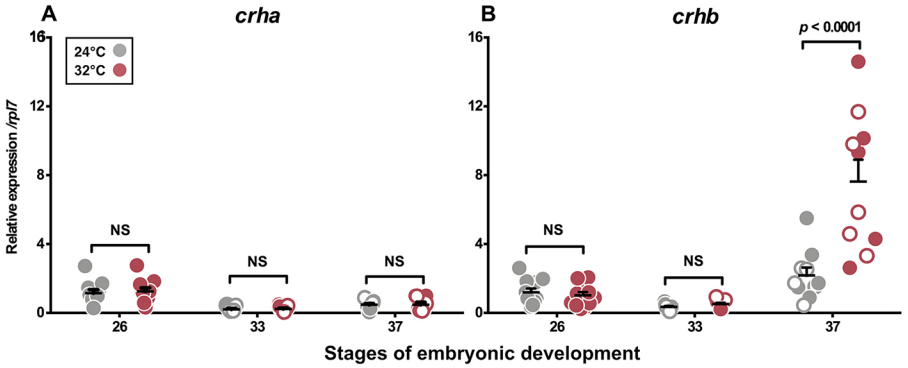

Fig. 1. *crhb* is upregulated by thermal stress during the gonadal sex determination period. (A,B) Developmental profiles of *crha* (A) and *crhb* (B) transcript abundance in embryos reared at 24°C (control temperature) and 32°C (high temperature). Data were measured by qPCR analysis in whole embryos at stages 26, 33 and 37. Gene expression levels are expressed relative to the stage 26 group with 24°C treatment. Quantification was performed using the $2^{-\Delta\Delta Ct}$ method and values were normalized to *rpl7*. Genotypic sex was determined at stages 33 and 37 by the presence/absence of the *dmy* gene; XX and XY are represented by filled circles and open circles, respectively. Horizontal bars indicate mean, with its respective s.e.m. *P*-values are indicated when transcript abundance between temperature treatments at the same developmental stage differ statistically (REST; $P<0.05$). NS, not statistically significant.

determination period (Fig. 1B). It is noteworthy that the expression levels of both *crha* and *crhb* were not affected by the sex genotype (XX versus XY) (Fig. S1).

Based on the upregulation of *crhb* at stage 37 in embryos incubated at HT, we analyzed the transcript abundance of other HPI-related genes, such as the Crh receptor genes *crhr1* and *crhr2*; the three urocortins, urocortin [Ucn; also known as sauvagine (Svg) and urotensin 1 (Uts1)], urocortin 2 (Ucn2) and urocortin 3 (Ucn3) (Fig. 2A) (Hosono et al., 2017); and *acth* (Liu et al., 2003). The expression of both *crhr1* and *crhr2* (Fig. 2E,F), was upregulated at HT. No significant differences were observed in the transcript abundance of the other Crh-like genes, i.e. *uts1*, *ucn2* and *ucn3* (Fig. 2B-D), or *acth* (Fig. 2G), suggesting that these HPI axis-related genes are not regulated at the transcriptional level during exposure to thermal stress in early development.

Generation of biallelic mutation of *crhr1* and *crhr2* using CRISPR/Cas9 technology

To analyze the participation of the HPI axis in temperature-induced masculinization, we disrupted this axis through biallelic mutations (indels in F0 individuals created by injecting *cas9* and sgRNA) of *crhr1* or/and *crhr2* using CRISPR/Cas9 technology. Biallelic mutations of both Crh receptors generated indels in the transmembrane domain resulting in a receptor with a protein segment that fails to anchor into the membrane lipid bilayer, and is therefore unable to activate the intracellular G protein (Grammatopoulos, 2012). Thus, the sgRNAs for *crhr1* and *crhr2* genes were designed at exons 7 (located in transmembrane helix 3) and 10 (located in transmembrane helix 6; Fig. S2A), respectively. These sgRNAs were synthesized *in vitro*, and co-injected with *nCas9n* RNA (*cas9*) into one-cell-stage embryos. The mutagenesis efficiency

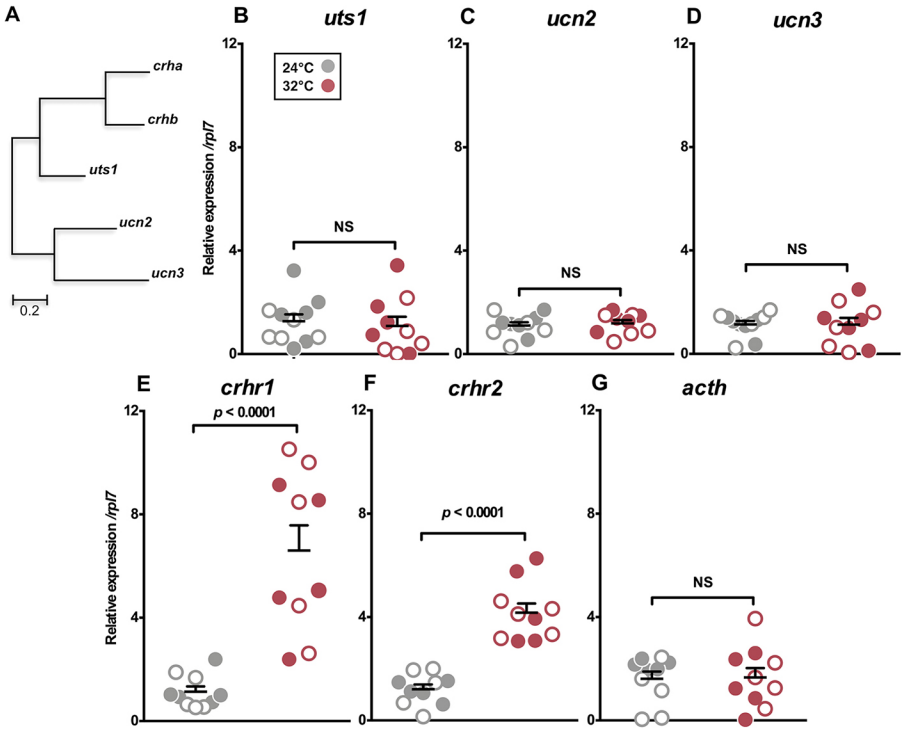

Fig. 2. Regulation of HPI-related genes during the gonadal sex determination period under HT treatment. (A) Phylogenetic tree showing the relationship among Crh family peptides in medaka, obtained using the neighbor-joining method and a bootstrap test (MEGA 7.0 software). The scale beneath the tree reflects sequence distances. Genbank accession sequences are provided in Table S1. (B-G) Gene expression profiles of urocortins (B-D), Crh receptors (E,F) and *acth* (G) in XX (filled circles) and XY (open circles) embryos reared at 24°C and 32°C. These data were measured by qPCR analysis in whole embryos at stage 37. Gene expression levels are expressed relative to the 24°C treatment. Quantification was performed using the $2^{-\Delta\Delta Ct}$ method and values were normalized to *rpl7*. Genotypic sex was determined by the presence/absence of the *dmy* gene; XX and XY are represented by filled circles and open circles, respectively. Horizontal bars indicate mean, with its respective s.e.m. *P*-values are indicated when transcript abundance between temperature treatments at the same developmental stage differ statistically (REST; $P<0.05$). NS, not statistically significant.

Development (2019) 146, dev172866. doi:10.1242/dev.172866

for each sgRNA was analyzed by a heteroduplex mobility assay (HMA; Fig. S2B) (Ota et al., 2013), which reached 96.6% (29/30; embryos with biallelic mutations/total of eggs injected) for sgRNA-*crhr1* and 100% (30/30) for sgRNA-*crhr2* (Fig. S3A,B). Also, biallelic mutants were mated with wild-type fish to generate F1 and then each Crh receptor was sequenced to confirm presence of the indels (Fig. S2C). Data indicate that most cells contained biallelic indels and, consequently, loss of function in *crhr1* and *crhr2* mutants. None of the embryos analyzed presented indels at the off-target sites for each of the injected sgRNAs of biallelic mutants (Fig. S3A,B).

Furthermore, no alterations in morphology or survival rate were observed in a batch of biallelic mutant animals reared at 24°C (CT) up to 60 days post-hatching (dph) (Fig. S4).

Genotypic female biallelic Crh receptor mutants did not show HT-induced masculinization

In order to assess the participation of Crh-related genes in the sex reversal of genotypic females to phenotypic males induced by HT, we analyzed the expression of well-known gene markers for gonadal sex differentiation in fish, such as *gsdf*, sry-box9 type 2α (*sox9a2*), gonadal aromatase (*cyp19a1a*, the gene encoding the aromatase enzyme involved in the synthesis of estrogen) and hydroxysteroid 11-beta dehydrogenase 2 (*hsd11b2*, the gene encoding the 11 beta-hydroxysteroid dehydrogenase, 11β-HSD, which catalyzes the interconversion of cortisol and cortisone, and the synthesis of 11-oxygenated androgens) (Chakraborty et al., 2016; Fernandino et al., 2012; Imai et al., 2015; Kurokawa et al., 2007; Nakamura et al., 2012; Shibata et al., 2010; Zhang et al., 2016; Zhou et al., 2016). Fertilized eggs were co-injected with *cas9* RNA and sgRNA for each Crh receptor (*cas9*+sgRNA-*crhr1* or *cas9*+sgRNA-*crhr2*) alone or together (*cas9*+sgRNA-*crhr1*+-*crhr2*) and they were then incubated at HT (32°C). Control fertilized eggs were injected only with *cas9* and then incubated at CT and HT (*cas9*-24°C and *cas9*-32°C, respectively; Fig. 3A). In all treatments, genotypic females (XX) that presented indels were selected for analysis of gene expression at stage 37. As expected, *cas9*-32°C individuals presented higher levels of *gsdf* and *sox9a2*, and lower *cyp19a1a* expression levels compared with *cas9*-24°C individuals (Fig. 3B-D), evidencing the molecular mechanism of action of masculinization induced by HT. However, the double biallelic Crh receptor mutants of genotypic females at HT showed a female pattern of lower *gsdf* and *sox9a2* and higher *cyp19a1a* expression levels, resembling those of the *cas9*-24°C group (Fig. 3B-D).

When each biallelic Crh receptor mutant of XX embryos was analyzed, the gene expression pattern showed an intermediate phenotype, with high *gsdf*, *sox9a2* and *cyp19a1a* (Fig. 3B-D). Here, it is necessary to take into account that in the biallelic mutant of each Crh receptor, the *crhr* paralog is fully active. We also analyzed the expression pattern of the androgen-related gene *hsd11b2*, which did not show differences between treatments (Fig. 3F).

Crh receptors are necessary to elicit sex reversal by high temperature

Besides the expression of testis and ovary-related gene markers, we also analyzed gonadal morphology of XX biallelic Crh receptor mutants that were incubated at CT and HT until hatching, and thereafter at 26°C (breeding temperature) for 20 dph, when the gonad could be morphologically well differentiated. Firstly, we analyzed the impact of biallelic mutation on the sex reversal of XX individuals incubated at 24°C injected with *cas9*, biallelic *crhr1*, *crhr2* and double Crh receptor mutants, in which no sex reversal individuals were found (Fig. 4A,B). In XX juveniles injected with *cas9* (control) and incubated at HT until hatching, 68.8% exhibited sex reversal, as evidenced by testis morphology (Fig. 4A,C). The double biallelic Crh receptor mutants showed a wide-ranging insensitivity to HT-induced female-to-male sex reversal, with nearly all XX individuals presenting normal ovary morphology (Fig. 4A,B). Moreover, 19% of the biallelic *crhr1* mutants exhibited sex reversal (Fig. 4A,C). However, 9.25% were presumptive intersex individuals, i.e. animals with ovaries containing spermatocytes (ova-testis; Fig. 4D). Finally,

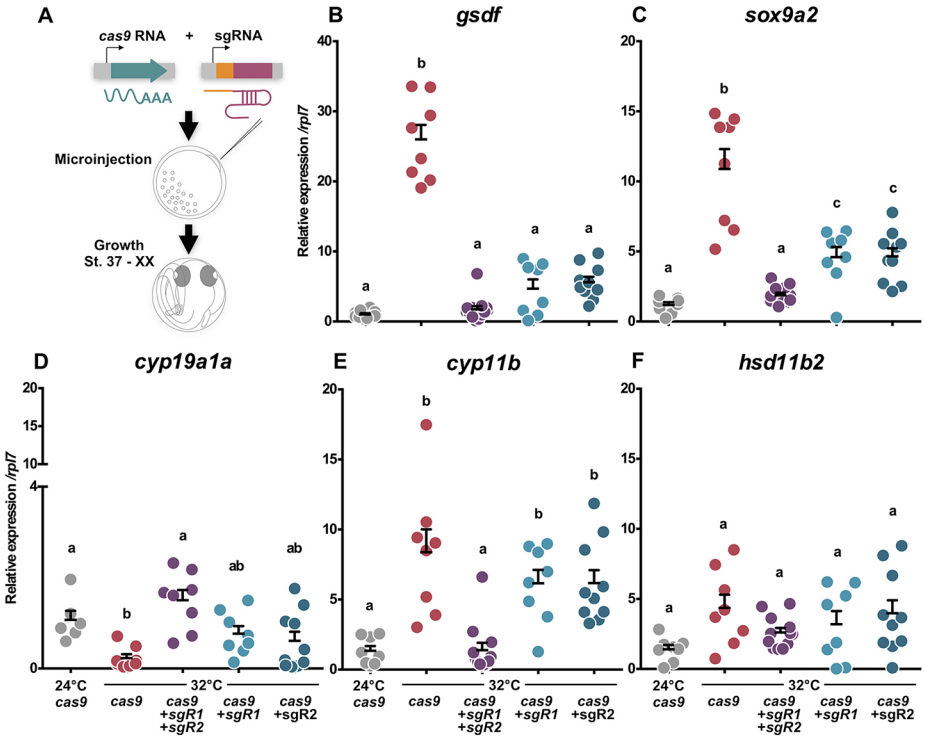

Fig. 3. Genotypic female biallelic Crh receptor mutants did not show HT-induced masculinization. (A) Schematic of the experimental procedure used to analyze the effect of loss of function of Crh receptors. (B-F) Transcript abundance profiles of the testicular genes markers *gsdf* and *sox9a2* (B,C), the ovarian gene marker *cyp19a1a* (D), the interrenal gland gene marker *cyp11b* (E) and the androgen-related gene *hsd11b2* (F), in control (*cas9*-injected embryos reared at 24°C and 32°C) and biallelic Crh receptor mutants (*cas9*+sgRNA-*crhr1*, *cas9*+sgRNA-*crhr2* and *cas9*+sgRNA-*crhr1*+-*crhr2* co-injected embryos reared at 32°C). These data were measured by qPCR analysis in whole embryos with genotypic sex XX at stage 37. Gene expression levels are expressed relative to the *cas9*-injected 24°C treatment group. Quantification was performed using the $2^{-\Delta\Delta Ct}$ method and values were normalized to *rpl7*. Horizontal bars indicate mean, with its respective s.e.m. Different letters indicate statistically significant differences between treatments (one-way ANOVA, followed by Tukey's multiple comparison test; $P<0.05$).

Development (2019) 146, dev172866. doi:10.1242/dev.172866

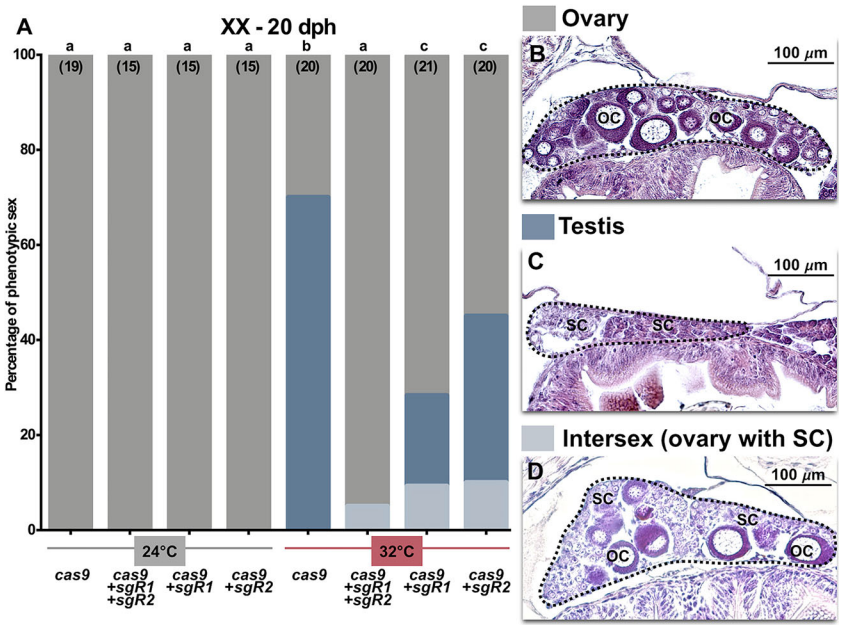

Fig. 4. Participation of Crh receptors in the sex reversal induced by HT. (A) Percentages of genetic females (XX) exhibiting different gonadal morphologies – ovary (gray), testis with spermatocytes (dark blue), intersex (oocytes with spermatocytes; light blue) – in embryos injected with *cas9* (control), *cas9*+sgRNA-*crhr1*, *cas9*+sgRNA-*crhr2* and *cas9*+sgRNA-*crhr1*+sgRNA-*crhr2*. The number of medaka juveniles analyzed in each treatment is shown in parentheses. Different letters indicate statistically significant differences between treatments (hypothesis testing to compare two population proportions, Z-test, $P<0.05$). (B-D) Examples of the different gonadal morphologies observed. OC, oocytes; SC, spermatocytes.

in XX biallelic *crhr2* mutant juveniles 35% presented sex reversal and 10% had intersex gonads (Fig. 4A,C,D).

Biallelic mutations of Crh receptors result in inhibition of Acth release and lack of cortisol increase

As we previously did not observe a correlation between the upregulation of *crhb* and the abundance of *acth* transcripts (Figs 1 and 2), we measured Acth-immunoreactive (Acth-ir) cells using immunofluorescence in the pituitary of genotypic female embryos at stage 39, with or without functional receptors, incubated at CT or HT (Fig. 5A). Firstly, we observed differences in the fluorescence intensity of the Acth-ir cells in XX embryos incubated at control and high temperature (Fig. 5B,C,H), suggesting that thermal stress induces Acth release. Moreover, we measured Acth-ir in biallelic Crh receptor mutants and observed higher fluorescence intensity compared with *cas9* embryos incubated at HT (Fig. 5C-F, Fig. S5), resembling the XX *cas9* control (24°C) embryos (Fig. 5B, Fig. S5). These results show that the biallelic mutation of Crh receptors in XX embryos causes accumulation of Acth in pituitary cells, indicating that both Crh receptors are involved in Acth release in the stress response induced by high temperature.

To corroborate that biallelic mutations of Crh receptors do disrupt the HPI axis, the level of cortisol and the mRNA expression of P450 11-beta (*cyp11b*), an enzyme expressed by the interrenal gland and involved in cortisol synthesis (Montero et al., 2015), were measured in all treatment groups. We observed in both biallelic *crhr1* and *crhr2* mutants an increase of cortisol levels at the end of the gonadal sex determination period, whereas the levels of cortisol in the double biallelic Crh receptor mutants were completely suppressed (Fig. 5H). Additionally, *cyp11b* was upregulated at HT but downregulated in the double biallelic Crh receptor mutants to low transcriptional levels similar to those observed at the control temperature (Fig. 3E), showing that the pathway involved in the synthesis of cortisol is transcriptionally active.

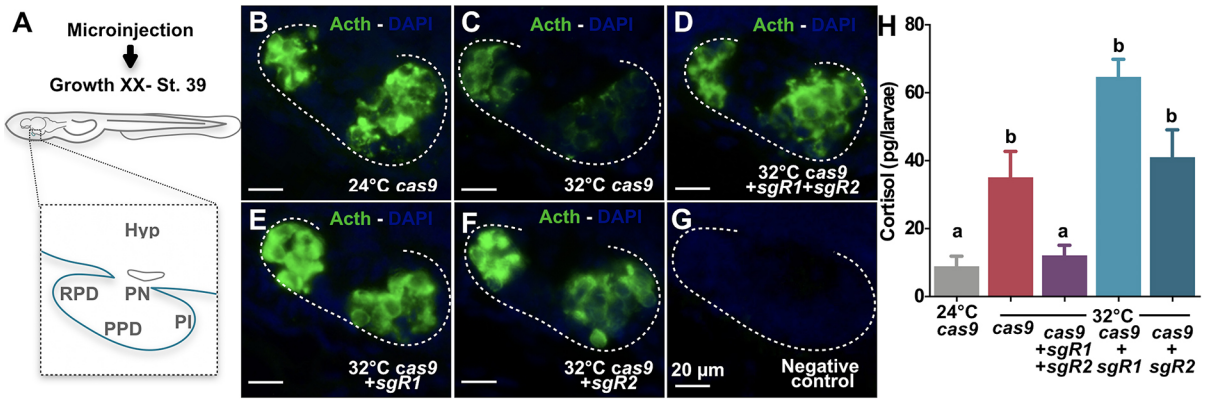

Fig. 5. Biallelic mutations of Crh receptors inhibit Acth release, losing the increase of cortisol induced by HT. (A) Schematic of the pituitary gland. Hyp, hypothalamus; PI, pars intermedia; PN, pars nervosa; PPD, proximal pars distalis; RPD, rostral pars distalis. (B-F) Fluorescent images of Acth-ir cells in the pituitary of embryos injected with *cas9* RNA at 24°C (B), *cas9* RNA at 32°C (C), and *cas9*+sg*crhr1*+sg*crhr2* (D), *cas9*+sg*crhr1* (E) and *cas9*+sg*crhr2* (F) co-injected embryos reared at 32°C until stage 39. (G) Negative control (incubation with secondary antibody alone). (H) Quantification of cortisol levels in embryos injected with *cas9* (controls at 24°C and 32°C), *cas9*+sgRNA-*crhr1*, *cas9*+sgRNA-*crhr2* or *cas9*+both Crh receptor sgRNAs at 32°C. Horizontal bars indicate mean, with its respective s.e.m. Different letters indicate statistically significant differences between treatments (one-way ANOVA, followed by Tukey's multiple comparison test; $P<0.05$).

Development (2019) 146, dev172866. doi:10.1242/dev.172866

Cortisol exposure rescued the lack of a sex reversal phenotype in Crh receptor mutants

In view of the fact that the entire HPI axis seems to be functional during the crucial period of gonadal fate and the biallelic mutations in Crh receptors inhibited masculinization of genotypic females incubated at HT, we decided to test whether the addition of cortisol could rescue the absence of sex reversal in the mutants. Therefore, we performed an experiment in which all embryos were maintained in an embryo medium with or without cortisol (5 µM) from fertilization to 5 dph (Fig. 6A) (Hayashi et al., 2010). The double biallelic Crh receptor mutants exhibited transcription consistent with the phenotype of XX at HT, with a low transcript abundance of *gsdf* (Fig. 6B), i.e. a typical XX-24°C *gsdf* expression pattern.

Finally, XX biallelic *crhr1* mutants, treated with or without cortisol at HT, presented high levels of *gsdf*, similar to those of control XX *cas9*-injected larvae (Fig. 6B), suggesting that the XX biallelic *crhr1* mutation is not sufficient to induce a female (low) pattern of *gsdf*. These results are in agreement with the high level of cortisol observed at stage 39 (Fig. 5H). However, XX biallelic *crhr2* mutant larvae reared at HT maintained low transcript abundance of *gsdf* (Fig. 6B), a typical female-like expression pattern. Most importantly, XX biallelic *crhr2* mutants reared with 5 µM cortisol at HT showed a male-like (high) *gsdf* expression pattern, similar to that of XX *cas9*-injected XX fish (Fig. 6B). To better understand the compensatory molecular mechanism, we analyzed the transcript abundance of *crhr2* and *crhr1* in the XX biallelic *crhr1* and *crhr2* mutants, respectively. We observed upregulation of *crhr2* in the XX biallelic *crhr1* mutants (Fig. 6C), but not of *crhr1* in XX biallelic *crhr2* mutant larvae (Fig. 6D), suggesting a molecular compensatory mechanism.

DISCUSSION

Environmental factors that act during the crucial period of fish gonadal development are able to alter sex ratios, especially toward males (Fernandino et al., 2013; Ospina-Álvarez and Piferrer, 2008). Despite established genotypic sex-determining mechanisms with known sex-determining genes, many fish species produce male-skewed sex ratios when environmental temperatures are elevated during early development. However, whether this phenomenon has any adaptive value or not is unknown for the vast majority of species. Although understanding of this mechanism is of great interest for basic biology and from the perspective of global climate change, the pathways that mediate environmental cues and gonadal fate, and the involvement of extra-gonadal organs in this process, are still unknown. Our results demonstrate for the first time the fundamental role of the CNS as the transducer in a form of environmental sex determination (ESD), through regulation of the HPI axis.

In the current work we demonstrated that, during the gonadal sex determination period, the HPI axis is active. Moreover, we proved that out of two *crh* paralogs, only *crhb* was upregulated at high masculinizing temperatures along embryonic development. In medaka, the *crha* gene was previously misidentified as a new member of Crh family and named as *telocortin* (*tcn*). The expression of *crha* has been mainly observed in the retina, with a weak expression in the brain (Hosono et al., 2015). In another teleost, *Astatotilapia burtoni*, the presence of *crha* has been related to the mediation of social information or stress responses in the visual system, facilitating signal processing before it even reaches the brain (Grone and Maruska, 2015). These previous results are in concordance with our observation that *crha* transcription does not seem to be induced by environmental stressors, such as high temperature. Besides *crha* and *crhb*, other members of the Crh gene

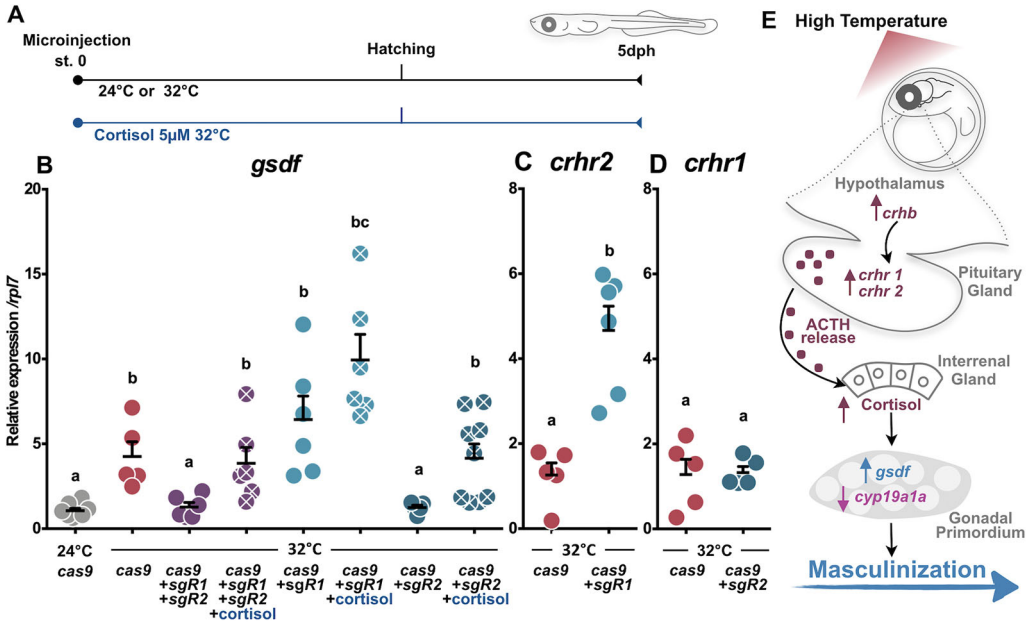

Fig. 6. Rescue of masculinization in biallelic Crh receptor mutants by cortisol treatment. (A) Schematic of the experimental procedure. (B) Gene expression profile of the testicular gene marker *gsdf* was analyzed in embryos injected with *cas9* (control), *cas9*+sgRNA-*crhr1*, *cas9*+sgRNA-*crhr2* and *cas9*+sgRNA-*crhr1*+sgRNA-*crhr2* then treated with cortisol (5 µM) or vehicle (ethanol) between fertilization and 5 dph at 32°C. (C,D) Quantification of *crhr2* (C) and *crhr1* (D) expression in *cas9*+sgRNA-*crhr1* and -*crhr2* co-injected larvae, respectively. Gene expression levels are expressed relative to *cas9*+sgRNA-*crhr1* without cortisol treatment (in B) and to *cas9* treatment (in C,D). Data were measured by qPCR in whole embryos with the genotypic sex XX. Quantification was performed using the $2^{-\Delta\Delta Ct}$ method and values were normalized to *rpl7*. Horizontal bars indicate mean, with its respective s.e.m. Different letters indicate statistically significant differences between treatments (REST; $P<0.05$). (E) Schematic of the proposed mechanism by which the CNS, through corticotropin-releasing hormone b (*crhb*) and its receptors (*crhr1* and *crhr2*), transduces stress-induced masculinization.

Development (2019) 146, dev172866. doi:10.1242/dev.172866

family are present in the medaka genome, such as the *uts1*, *ucn2* and *ucn3* (Hosono et al., 2017). Known as urocortins, these genes code for neuropeptides that share structural similarity with Crh proteins and can act as additional endogenous ligands for Crh receptors. In mice, they have been involved in stress responses and also anxiety (Bale and Vale, 2004; Sztainberg and Chen, 2012). Nevertheless, none of the urocortins was upregulated during the sex determination period at high, masculinization temperature.

The high expression of *crhb* we observed at HT is in agreement with results of other well-known stress responses, including its role in regulating the release of glucocorticoids (Alderman and Bernier, 2009; Carpenter et al., 2014; Chen and Fernald, 2008; Grone and Maruska, 2015). Moreover, a similar pattern was obtained for the Crh receptors (*crhr1* and *crhr2*), which are crucial for activation of the HPI axis (Lovejoy and de Lannoy, 2013) during the gonadal sex determination period. In medaka, the first peak of cortisol occurs in 2 dph larvae, when animals are reared at normal breeding temperatures (Trayer et al., 2013). However, Hayashi et al. (2010) and our study showed an early rise in cortisol in embryos reared at HT, at the time of the gonadal sex determination period, evidencing an earlier activation of mechanisms involved in the surge of cortisol levels. In this regard, the high expression of *crhb* and the receptors *crhr1* and *crhr2* in our study is consistent with the timing of cortisol increase. Notably, overlap between the timing of early activation of the HPI axis and the gonadal sex determination period is crucial for understanding how high levels of cortisol are triggered and are related to male-skewed sex ratio (Hattori et al., 2009; Hayashi et al., 2010). Subsequently, in order to validate our hypothesis, we disrupted the HPI axis with biallelic mutation of both Crh receptors. These mutants were characterized by a lack of cortisol response at HT, downregulation of testicular gene markers, and concomitant inhibition of sex reversal (masculinization in XX) induced by stress. Thus, double biallelic Crh receptor mutants phenocopied the previous results on the inhibition of cortisol synthesis, with the absence of sex reversal in genotypic females (Hayashi et al., 2010). These observations demonstrate for the first time participation of the brain in stress-induced masculinization.

In all vertebrates, Crh regulates the synthesis and release of Acth (Mommsen et al., 1999; Wendelaar Bonga, 1997) through their transmembrane receptors in the pituitary gland (Lovejoy et al., 2014). In the present work, although *acth* transcript abundance did not show any change during the gonadal sex determination period and under stress conditions, we detected low intensities of Acth-ir in HT embryos, which could be explained by a stimulation of Acth release, or the lack of peptide synthesis (Aguilera and Liu, 2012; Kovács, 2013), induced by thermal stress. Moreover, biallelic mutations of both Crh receptors resulted in more Acth in the pituitary, phenocopying the high fluorescence pattern of the control group. Furthermore, this Acth accumulation and/or the lack of its release are in concordance with the complete suppression of cortisol levels observed in the loss-of-function Crh receptor mutants. Therefore, the strong decrease in cortisol level of the double Crh receptor mutants resembled the absence of a stress response observed without an environmental stressor, with the concomitant absence of female sex reversal. In addition, the double Crh receptor mutant phenocopied previous results observed after inhibition of cortisol synthesis in medaka (Hayashi et al., 2010), with the absence of sex reversal. Such disruption of the HPI axis was demonstrated to be crucial for female-to-male sex reversal in our studies with medaka under high, stressful temperatures.

An in-depth analysis of the molecular responses to loss of function of each Crh receptor under thermal stress showed that, whereas embryos co-injected with *cas9*+sgRNA-*crhr1* or *crhr2* presented an early inhibition of *gsdf* expression, high Acth-ir intensity and body cortisol level were observed at the end of the gonadal sex determination period when only one of the Crh receptor genes was biallelically mutated. Initially, it is necessary to take into account that in each biallelic Crh receptor mutant the paralog is fully active, which would generate a late compensatory effect, explaining the late high levels of cortisol at the end of the gonadal sex determination period, with the concomitant partial rescue of the sex reversal. Nevertheless, the regulatory mechanism of each biallelic Crh receptor mutant differs. In the biallelic *crhr1* mutants, a transcriptional compensatory effect was observed with the upregulation of *crhr2*, which could establish the high Acth-ir intensity and cortisol level. However, in the biallelic *crhr2* mutants, the transcription of *crhr1* did not change. Therefore, the high Acth-ir intensity in these *crhr1* biallelic mutants could be explained by a late inhibition of Acth release, leading to a high level of cortisol. In mammals, both Crh and Crhr1 are associated with the HPA axis at the initial stress response, whereas Crhr2 plays a major role during chronic and later responses to stress (Lovejoy and de Lannoy, 2013). *Crhr1* knockout mice showed reduced stress-induced release of Acth and corticosterone, providing evidence that Crhr1 mediates stress-induced hormone activation (Smith et al., 1998; Timpl et al., 1998). On the other hand, *Crhr2*-deficient mice exhibited hypersensitivity of the HPA axis to stress (Bale et al., 2000), presenting a later decrease of plasma Acth and an increase of corticosterone, suggesting that Crhr2 is also involved in the maintenance of HPA axis drive (Coste et al., 2000). In view of these considerations, our data showing the loss of *crhr2* function provide a similar regulatory mechanism to that reported in mice, resulting in a late decrease of Acth release, but with a high level of cortisol. Nevertheless, the loss of *crhr1* function in medaka presented a novel molecular compensatory mechanism: upregulation of *crhr2*, promoting late synthesis of Acth, with a concomitant high level of cortisol. Taken together, these results highlight the importance of the involvement of both Crh receptors in fish masculinization induced by environmental stressors.

Once the HPI axis has translated the stimulus of an environmental stressor, is important to know how cortisol transduces this response to masculinize the gonad. In some fish, including medaka, it has been proposed that gonadal aromatase, an enzyme involved in estradiol synthesis, or other genes related to its regulation, such as FTZ-F1 (the ortholog of mammalian steroidogenic factor1), are inhibited by cortisol (Hayashi et al., 2010; Navarro-Martín et al., 2011; Yamaguchi et al., 2010). Furthermore, in pejerrey (*Odontesthes bonariensis*) it has been suggested that androgens, synthesized through the action of *hsd11b2*, are considered as mediators of stress (Fernandino et al., 2012, 2013). Our results confirm that *cyp19a1a* transcription is suppressed at HT and demonstrate that high transcription levels can be rescued in double biallelic Crh receptor mutants.

Three different results – (1) disruption of the HPI axis, (2) the increase of testicular gene markers with the concomitant decrease of sex reversal of genotypic females, and (3) the rescue of masculinization with cortisol – support the fact that the CNS is involved in sex reversal induced by environmental stressors (as summarized in Fig. 6E), in contrast to genotypic sex determination in which the sexual fate decision begins from the gonad.

MATERIALS AND METHODS

Source of animals and experimental conditions

Fertilized eggs of *Oryzias latipes* were incubated in 70 mm Petri dishes with embryo medium (17 mM NaCl, 0.4 mM KCl, 0.27 mM $CaCl_2.2H_2O$ and

Development (2019) 146, dev172866. doi:10.1242/dev.172866

0.66 mM $MgSO_4$; pH 7) at 24°C (CT) or 32°C (HT). Sampling was performed at stages 26, 33, 37 and 39, and at 5, 20 or 60 days post-hatching (dph) (Iwamatsu, 2004). These stages correspond to the end of primordial germ cell (PGC) migration and the formation of the gonadal primordium (stage 26), the beginning of *dmy/dmrt1bY* transcription in gonadal somatic cells (stage 33), the sexual dimorphism in PGC proliferation (stage 35-37), and to the maximum PGCs proliferation in XX embryos and latest embryo stage of the gonadal sex determination period (stage 39) (Saito et al., 2007). Based on previous work, we know that 5-dph larvae are sensitive to cortisol treatment (Hayashi et al., 2010), that 20-dph fish can easily be assessed for gonadal sex morphology, and that 60-dph animals have grown as adult fish so can be used to assess survival. The strain hi-medaka (ID: MT835) was supplied from the National BioResource Project (NBRP) Medaka (www.shigen.nig.ac.jp/medaka/). All fish were maintained and fed following standard protocols to medaka (Kinoshita et al., 2012). Fish were handled in accordance with the Universities Federation for Animal Welfare Handbook on the Care and Management of Laboratory Animals (www.ufaw.org.uk) and internal institutional regulations.

RNA and quantification by RT-qPCR

Total RNA was extracted from individual embryos using the RNAqueous-Micro kit (Ambion by Life Technologies) for stage 26, the Illustra RNAspin Mini for stage 33, and 350 µl of TRIzol Reagent (Life Technologies) for stages 37, 39 and 5 dph, following the manufacturer's instructions. To perform cDNA synthesis, RNA of each individual sample (250 ng) was treated with Deoxyribonuclease I Amplification Grade (Life Technologies) and reverse-transcribed using SuperScript II (Life Technologies) with oligo(dT) following the manufacturer's instructions. Each primer pair was previously validated by analyzing the melting curve, requiring an efficiency of 95-105%, with a slope of around −3.30 and R2 value>0.99. Real-time PCR primers are listed in Table S1. Samples were analyzed with the Step One Plus Real-Time PCR System (Applied Biosystems). The amplification protocol consisted of an initial cycle of 1 min at 95°C, followed by 10 s at 95°C and 30 s at 60°C for a total of 45 cycles. The subsequent quantification method was performed using the $2^{-\Delta\Delta Ct}$ method (threshold cycle; assets.thermofisher.com/TFS-Assets/LSG/manuals/cms_040980.pdf) and normalized against reference gene values for ribosomal protein L7 (*rpl7*) (Zhang and Hu, 2007).

Sexing of embryos by PCR

Each embryo of stages 33, 37 and 39, and each 5-dph and 20-dph larva was analyzed to determine its genotypic sex. Animals were subjected to DNA analysis for the presence of the *dmy/dmrt1bY* gene. For this purpose, we collected DNA from each RNA extraction following manufacturer's instructions. PCR analysis was then performed using primers for *dmy* (Nanda et al., 2002) and the presence of *β-actin* gene was used as a DNA loading control (Table S1) (Hattori et al., 2007). The PCR products were analyzed on a 1% agarose gel.

CRISPR/Cas9 target site design and single guide RNA (sgRNA) construction

CRISPR/Cas9 target sites were designed using the CCTop-CRISPR/Cas9 target online predictor (crispr.cos.uni-heidelberg.de/index.html) (Stemmer et al., 2015), which identified the sequences 5′GG-(N18)-NGG3′ in exon 7 of *crhr1* (TTGAGGAACATCATCCACTGG) and exon 10 of *crhr2* (GAGGCAGCAAGACGAGTGTGG) (Fig. S2A,C). Each sgRNA was synthesized by cloning the annealed oligonucleotides into the sgRNA expression vector pDR274 (Addgene #42250) (Hwang et al., 2013) followed by *in vitro* transcription, previously established by Ansai and Kinoshita (2014). Briefly, a pair of oligonucleotides at final concentration of 10 mM each was annealed in 10 ml of annealing buffer (40 mM Tris-HCl pH 8.0, 20 mM $MgCl_2$ and 50 mM NaCl) by heating to 95°C for 2 min and then cooling slowly to 25°C. Then, the pDR274 vector was digested with BsaI-HF (New England Biolabs), and the annealed oligonucleotides were ligated into the pDR274 vector. The sgRNA expression vectors were digested by DraI, and sgRNAs were synthesized using the MEGAshortscript T7 Transcription Kit (Thermo Fisher Scientific). The synthesized sgRNAs were purified by RNeasy Mini kit purification (Qiagen). These RNA sequences were diluted to 50 ng/µl.

Capped Cas9 RNA synthesis

The capped *cas9* (nCas9n RNA) was transcribed from pCS2-nCas9n plasmid (Addgene #47929). First, the plasmid was linearized by NotI and capped *cas9* was synthesized by mMESSAGE mMACHINE SP6 kit (Life Technologies). The synthesized *cas9* was purified by RNeasy Mini kit purification (Qiagen) and RNAs were diluted to 200 ng/µl.

Microinjection into embryos

Microinjection was performed into fertilized medaka eggs before the first cleavage as described previously (Kinoshita et al., 2000). For the CRISPR/Cas9 system, 25 ng/µl *sgRNA* and 100 ng/µl *cas9* were co-injected in 4.6 nl of RNA mixture. Embryos injected with *cas9* were used as controls. Microinjection was performed with a Nanoject II Auto-Nanoliter Injector (Drummond Scientific) coupled to a stereomicroscope (Olympus).

DNA extraction for heteroduplex mobility assay (HMA)

To analyze the efficiency and specificity of the CRISPR/Cas9 system, 3 days post-fertilization embryos were used (Ansai and Kinoshita, 2014). Genomic DNA was extracted by incubating each medaka embryo in 25 µl of 5 mM NaOH, 0.2 mM EDTA at 95°C for 5 min. After cooling to room temperature (RT) 25 µl of 40 mM Tris-HCl, pH 8.0, was added to the extract. The supernatant was used as template for PCR for HMA. Conventional PCR analysis was performed with genomic DNA using primers listed in Table S1. Electrophoresis was performed on 12% acrylamide gel (Ota et al., 2013); gels were stained with ethidium bromide for 15 min before examination. Multiple heteroduplex bands shown by HMA in PCR amplicons from each injected embryo were quantified as embryos with biallelic mutations, whereas single bands were quantified as no-edited embryos (Fig. S2B). The mutation rate was calculated as the ratio of the number of multiple heteroduplex bands shown in PCR amplicons from each Cas9-sgRNA-injected embryo to the sum of all embryos injected multiplied by 100 (n=30/per sgRNA) (Ansai and Kinoshita, 2014).

Off-target analysis

Potential off-target sites in the medaka genome for each sgRNAs were searched using a 'Pattern Match' tool in New Medaka Map (beta) at the NBRP medaka web site (http://viewer.shigen.info/medakavw/patternmatch) and CCTop-CRISPR/Cas9 target online predictor (Stemmer et al., 2015). All potential off-target sites identified were analyzed by HMA using the primers listed in Table S1.

Biallelic mutant screening

Finally, the screening of indels was performed in F1 fish. Biallelic mutant adult (F0) medaka were mated with wild-type medaka of the Himedaka strain (WT). Genomic DNA was extracted from each F1 embryo for analysis of mutations by HMA, as described previously (Table S1). Mutant alleles in each embryo were determined by direct sequencing of the *crhr1* or *crhr2* gene region.

Histological analysis

Samples for histological examination of gonadal sex (n=15-25/per group) were taken at 20 dph and analyzed following the criteria reported above. Firstly, the caudal fin was taken for gDNA extraction using conventional saline buffer extraction to determine genotypic sex and for HMA analysis (Aljanabi and Martinez, 1997). The body trunk was fixed in Bouin's solution and processed according to standard protocols for the preparation of Hematoxylin & Eosin-stained histological sections. These preparations were examined under a Nikon ECLIPSE Ni-U microscope (Nikon) and captured using a Digit Sight DS-Fi2 digital camera (Nikon).

Immunofluorescence analysis of Acth

Medaka embryos at stage 39 from different treatment groups were used. All individuals were processed under the same conditions for fixation, washing and incubation with serum and antibody. Stage 39 was chosen for analysis of the release of Acth upon upregulation of *crhb*, which was detected at stage 37. The tail was used for sex genotying by PCR and HMA analysis and the rest of the body was fixed in Bouin's solution overnight. Sections were then washed with 0.1 M phosphate-buffered saline (PBS pH 7.4) and blocked in

0.1 M PBS containing 0.5% bovine serum albumin (Sigma-Aldrich) for 60 min before overnight incubation with a mixture of primary antibody against ACTH-NIDDK-anti-hATCH-IC-3 (rabbit, 1:250; kindly provided by Dante Paz, Universidad de Buenos Aires) (Garrel et al., 2002) at RT. After incubation, the sections were washed twice in PBS for 10 min each and incubated at RT for 90 min with Alexa Fluor 488-conjugated secondary antibody goat anti-rabbit IgG (ThermoFisher Scientific, A-11008) at a dilution of 1:2000 in PBS. Separate sets of slides were treated only with secondary antibody (negative controls). After incubation, sections were rinsed twice with PBS and mounted with Fluoromount mounting medium (Sigma-Aldrich) containing 4′,6-diamidino-2-phenylindole (DAPI, 5 µg/ml, Life Technologies). Section photographs were taken using a Nikon Eclipse E7000 and Image Pro Plus (Media Cybernetics) with the same capture conditions of exposure and gain for all samples. Finally, images were analyzed and measured for fluorescence using ImageJ (https://imagej.nih.gov/ij/) using fluorescence intensity within the pituitary gland relative to mean background fluorescence.

Levels of cortisol

Enzyme immunoassay (EIA) was performed using the Cortisol Express EIA Kit according to instructions from the manufacturer (Cayman Chemical) and previously used by our group (Fernandino et al., 2012). Briefly, pools of 23-25 embryos of each treatment and from both sexes were frozen at −80°C, homogenized in 0.2 ml of PBS, and used for steroid extraction with 1 ml of diethyl ether. This procedure was repeated two times. After evaporation of the diethyl ether, samples were immediately re-suspended in 2 ml EIA buffer and analyzed in a microplate reader (Rayto Model RT-2100C) following the kit instructions. The recovery rate was estimated by the cold-spike method to be 0.85% and the intra- and inter-assay variation (CV%) ranged from 4 to 13%.

Rescue of biallelic mutant phenotype by cortisol treatment

Both *cas9*+sgRNA-*crhr1* and/or +sgRNA-*crhr2* co-injected fish were treated with 5 µM of cortisol (18) (11β-11,17,21-trihydroxypregn-4-ene-3,20-dione; Sigma-Aldrich) from fertilization to 5 dph. Briefly, after injection with a mixture of sgRNA (*crhr1* and/or *crhr2*) and *cas9*, the embryos were placed in a 70 mm Petri dish with embryo rearing medium (25 ml) supplemented with cortisol or vehicle control (with the same volume of stock solvent: 4.53 µl ethanol, 0.018%). The medium was changed every day. Both groups were reared at HT. Finally, gDNA and RNA were extracted, as explained above, from each embryo for genotypic sex and HMA analysis, and RT-qPCR analysis, respectively.

Statistical analysis

All values are presented as mean±s.e.m. Fold change and statistical analysis of RT-qPCR quantifications were performed using FgStatistics interface (http://sites.google.com/site/fgStatistics/), based on the Relative Expression Software Tool (REST) from Pfaffl et al. (2002). Immunohistochemistry quantification was analyzed by χ^2-distribution and statistical analyses were performed using SPSS v20 program, using one-way analysis of variance (ANOVA), followed by Tukey's multiple comparison test. Differences in sex ratio were determined by hypothesis test for differences in two population proportions, Z-test. All differences were considered statistically significant when $P<0.05$.

Acknowledgements

We thank Gabriela C. López (INTECH) for helping with histological and immunohistochemical preparations. We also thank Masato Kinoshita (Kyoto University) for teaching and helping with CRISPR/Cas9 technique, Adrián Mutto (Insituto de Investigaciones Biotecnológicas-UNSAM) for helping with microinjections, and Ricardo S. Hattori (Unidade de Pesquisa e Desenvolvimento de Campos do Jordão, APTA/SAA) for helpful advice. We are grateful to NBRP Medaka (https://shigen.nig.ac.jp/medaka/) for providing hi-medaka (Strain ID: MT835).

Competing interests

The authors declare no competing or financial interests.

Author contributions

Conceptualization: D.C.C.C., J.I.F.; Methodology: D.C.C.C., L.F.A.P., V.S.L., G.M.S., J.I.F.; Formal analysis: D.C.C.C., L.F.A.P., J.I.F.; Resources: J.I.F.; Writing - original draft: J.I.F.; Writing - review & editing: D.C.C.C., V.S.L., G.M.S., J.I.F.; Supervision: J.I.F.; Project administration: J.I.F.; Funding acquisition: V.S.L., G.M.S., J.I.F.

Funding

This work was supported by the Consejo Nacional de Investigaciones Científicas y Técnicas (CONICET) (D2979/16 to J.I.F., PhD scholarships to D.C.C.C. and L.F.A.P., and Scientific Researcher Career positions for J.I.F. and G.M.S.); by the Agencia Nacional de Promoción Científica y Tecnológica (grants 1565/14 and 2501/15 to J.I.F., and 2783/15 to G.M.S.); by a Discovery Grant from the Natural Sciences and Engineering Research Council of Canada (NSERC) (RGPIN 418576-2012 to V.S.L.); and by Canada Research Chairs (to V.S.L.).

Supplementary information

Supplementary information available online at http://dev.biologists.org/lookup/doi/10.1242/dev.172866.supplemental

References

Aguilera, G. and Liu, Y. (2012). The molecular physiology of CRH neurons. *Front. Neuroendocrinol.* **33**, 67-84. doi:10.1016/j.yfrne.2011.08.002

Alderman, S. L. and Bernier, N. J. (2009). Ontogeny of the corticotropin-releasing factor system in zebrafish. *Gen. Comp. Endocrinol.* **164**, 61-69. doi:10.1016/j.ygcen.2009.04.007

Aljanabi, S. M. and Martinez, I. (1997). Universal and rapid salt-extraction of high quality genomic DNA for PCR-based techniques. *Nucleic Acids Res.* **25**, 4692-4693. doi:10.1093/nar/25.22.4692

Ansai, S. and Kinoshita, M. (2014). Targeted mutagenesis using CRISPR/Cas system in medaka. *Biol. Open.* **3**, 362-371. doi:10.1242/bio.20148177

Backström, T. and Winberg, S. (2013). Central corticotropin releasing factor and social stress. *Front. Neurosci.* **7**, 117. doi:10.3389/fnins.2013.00117

Bale, T. L. and Vale, W. W. (2004). CRF and CRF receptors: role in stress responsivity and other behaviors. *Annu. Rev. Pharmacol. Toxicol.* **44**, 525-557. doi:10.1146/annurev.pharmtox.44.101802.121410

Bale, T. L., Contarino, A., Smith, G. W., Chan, R., Gold, L. H., Sawchenko, P. E., Koob, G. F., Vale, W. W. and Lee, K.-F. (2000). Mice deficient for corticotropin-releasing hormone receptor-2 display anxiety-like behaviour and are hypersensitive to stress. *Nat. Genet.* **24**, 410-414. doi:10.1038/74263

Bernier, N. J., Alderman, S. L. and Bristow, E. N. (2008). Heads or tails? Stressor-specific expression of corticotropin-releasing factor and urotensin I in the preoptic area and caudal neurosecretory system of rainbow trout. *J. Endocrinol.* **196**, 637-648. doi:10.1677/JOE-07-0568

Capel, B. (2017). Vertebrate sex determination: evolutionary plasticity of a fundamental switch. *Nat. Rev. Genet.* **18**, 675. doi:10.1038/nrg.2017.60

Carpenter, R. E., Maruska, K. P., Becker, L. and Fernald, R. D. (2014). Social opportunity rapidly regulates expression of CRF and CRF receptors in the brain during social ascent of a teleost fish, *Astatotilapia burtoni*. *PLoS ONE* **9**, e96632. doi:10.1371/journal.pone.0096632

Chakraborty, T., Zhou, L. Y., Chaudhari, A., Iguchi, T. and Nagahama, Y. (2016). Dmy initiates masculinity by altering Gsdf/Sox9a2/Rspo1 expression in medaka (*Oryzias latipes*). *Sci. Rep.* **6**, 19480. doi:10.1038/srep19480

Chandler, C. H., Phillips, P. C. and Janzen, F. J. (2008). The evolution of sex-determining mechanisms: lessons from temperature-sensitive mutations in sex determination genes in *Caenorhabditis elegans*. *J. Evol. Biol.* **22**, 192-200. doi:10.1111/j.1420-9101.2008.01639.x

Chandler, C. H., Chadderdon, G. E., Phillips, P. C., Dworkin, I. and Janzen, F. J. (2012). Experimental evolution of the Caenorhabditis elegans sex determination pathway. *Evolution* **66**, 82-93. doi:10.1111/j.1558-5646.2011.01420.x

Chen, C.-C. and Fernald, R. D. (2008). Sequences, expression patterns and regulation of the corticotropin-releasing factor system in a teleost. *Gen. Comp. Endocrinol.* **157**, 148-155. doi:10.1016/j.ygcen.2008.04.003

Coste, S. C., Kesterson, R. A., Heldwein, K. A., Stevens, S. L., Heard, A. D., Hollis, J. H., Murray, S. E., Hill, J. K., Pantely, G. A., Hohimer, A. R., et al. (2000). Abnormal adaptations to stress and impaired cardiovascular function in mice lacking corticotropin-releasing hormone receptor-2. *Nat. Genet.* **24**, 403-409. doi:10.1038/74255

Fernandino, J. I., Hattori, R. S., Kishii, A., Strüssmann, C. A. and Somoza, G. M. (2012). The cortisol and androgen pathways cross talk in high temperature-induced masculinization: 11β-hydroxysteroid dehydrogenase as a key enzyme. *Endocrinology* **153**, 6003-6011. doi:10.1210/en.2012-1517

Fernandino, J. I., Hattori, R. S., Moreno Acosta, O. D., Strüssmann, C. A. and Somoza, G. M. (2013). Environmental stress-induced testis differentiation: androgen as a by-product of cortisol inactivation. *Gen. Comp. Endocrinol.* **192**, 36-44. doi:10.1016/j.ygcen.2013.05.024

Garrel, G., Lozach, A., Bachir, L. K., Laverrière, J.-N. and Counis, R. (2002). Pituitary adenylate cyclase-activating polypeptide stimulates nitric-oxide synthase type I expression and potentiates the cGMP response to gonadotropin-releasing hormone of rat pituitary gonadotrophs. *J. Biol. Chem.* **277**, 46391-46401. doi:10.1074/jbc.M203763200

Ge, C., Ye, J., Weber, C., Sun, W., Zhang, H., Zhou, Y., Cai, C., Qian, G. and Capel, B. (2018). The histone demethylase KDM6B regulates temperature-dependent sex determination in a turtle species. *Science.* **360**, 645-648. doi:10.1126/science.aap8328

Grammatopoulos, D. K. (2012). Insights into mechanisms of corticotropin-releasing hormone receptor signal transduction. *Br. J. Pharmacol.* **166**, 85-97. doi:10.1111/j.1476-5381.2011.01631.x

Grammatopoulos, D. K. and Chrousos, G. P. (2002). Functional characteristics of CRH receptors and potential clinical applications of CRH-receptor antagonists. *Trends Endocrinol. Metab.* **13**, 436-444. doi:10.1016/S1043-2760(02)00670-7

Grone, B. P. and Maruska, K. P. (2015). Divergent evolution of two corticotropin-releasing hormone (CRH) genes in teleost fishes. *Front. Neurosci.* **9**, 365. doi:10.3389/fnins.2015.00365

Hattori, R. S., Gould, R. J., Fujioka, T., Saito, T., Kurita, J., Strüssmann, C. A., Yokota, M. and Watanabe, S. (2007). Temperature-dependent sex determination in Hd-rR medaka *Oryzias latipes*: gender sensitivity, thermal threshold, critical period, and DMRT1 expression profile. *Sex. Dev.* **1**, 138-146. doi:10.1159/000100035

Hattori, R. S., Fernandino, J. I., Kishii, A., Kimura, H., Kinno, T., Oura, M., Somoza, G. M., Yokota, M., Strüssmann, C. A. and Watanabe, S. (2009). Cortisol-induced masculinization: does thermal stress affect gonadal fate in pejerrey, a teleost fish with temperature-dependent sex determination? *PLoS ONE* **4**, e6548. doi:10.1371/journal.pone.0006548

Hayashi, Y., Kobira, H., Yamaguchi, T., Shiraishi, E., Yazawa, T., Hirai, T., Kamei, Y. and Kitano, T. (2010). High temperature causes masculinization of genetically female medaka by elevation of cortisol. *Mol. Reprod. Dev.* **77**, 679-686. doi:10.1002/mrd.21203

Holsboer, F. and Ising, M. (2008). Central CRH system in depression and anxiety - evidence from clinical studies with CRH1 receptor antagonists. *Eur. J. Pharmacol.* **583**, 350-357. doi:10.1016/j.ejphar.2007.12.032

Hosono, K., Kikuchi, Y., Miyanishi, H., Hiraki-Kajiyama, T., Takeuchi, A., Nakasone, K., Maehiro, S. and Okubo, K. (2015). Teleocortin: a novel member of the CRH family in teleost fish. *Endocrinology* **156**, 2949-2957. doi:10.1210/en.2015-1042

Hosono, K., Yamashita, J., Kikuchi, Y., Hiraki-Kajiyama, T. and Okubo, K. (2017). Three urocortins in medaka: identification and spatial expression in the central nervous system. *J. Neuroendocrinol.* **29**, 1-11. doi:10.1111/jne.12472

Hwang, W. Y., Fu, Y., Reyon, D., Maeder, M. L., Tsai, S. Q., Sander, J. D., Peterson, R. T., Yeh, J.-R. J. and Joung, J. K. (2013). Efficient genome editing in zebrafish using a CRISPR-Cas system. *Nat. Biotech.* **31**, 227-229. doi:10.1038/nbt.2501

Imai, T., Saino, K. and Matsuda, M. (2015). Mutation of Gonadal soma-derived factor induces medaka XY gonads to undergo ovarian development. *Biochem. Biophys. Res. Co.* **467**, 109-114. doi:10.1016/j.bbrc.2015.09.112

Iwamatsu, T. (2004). Stages of normal development in the medaka *Oryzias latipes*. *Mech. Dev.* **121**, 605-618. doi:10.1016/j.mod.2004.03.012

Kinoshita, M., Kani, S., Ozato, K. and Wakamatsu, Y. (2000). Activity of the medaka translation elongation factor 1α-A promoter examined using the GFP gene as a reporter. *Dev. Growth Differ.* **42**, 469-478. doi:10.1046/j.1440-169x.2000.00530.x

Kinoshita, M., Murata, K., Naruse, K. and Tanaka, M. (2012). *Medaka: Biology, Management, and Experimental Protocols*. Iowa, USA: Wiley-Blackwell.

Kitano, T., Hayashi, Y., Shiraishi, E. and Kamei, Y. (2012). Estrogen rescues masculinization of genetically female medaka by exposure to cortisol or high temperature. *Mol. Reprod. Dev.* **79**, 719-726. doi:10.1002/mrd.22080

Kovács, K. J. (2013). CRH: the link between hormonal-, metabolic- and behavioral responses to stress. *J. Chem. Neuroanat.* **54**, 25-33. doi:10.1016/j.jchemneu.2013.05.003

Kurokawa, H., Saito, D., Nakamura, S., Katoh-Fukui, Y., Ohta, K., Baba, T., Morohashi, K. and Tanaka, M. (2007). Germ cells are essential for sexual dimorphism in the medaka gonad. *Proc. Natl. Acad. Sci. USA* **104**, 16958-16963. doi:10.1073/pnas.0609932104

Liu, N.-A., Huang, H., Yang, Z., Herzog, W., Hammerschmidt, M. and Lin, S. (2003). Pituitary corticotroph ontogeny and regulation in transgenic zebrafish. *Mol. Endocrinol.* **17**, 959-966. doi:10.1210/me.2002-0392

Lovejoy, D. A. and de Lannoy, L. (2013). Evolution and phylogeny of the corticotropin-releasing factor (CRF) family of peptides: expansion and specialization in the vertebrates. *J. Chem. Neuroanat.* **54**, 50-56. doi:10.1016/j.jchemneu.2013.09.006

Lovejoy, D. A., Chang, B. S. W., Lovejoy, N. R. and del Castillo, J. (2014). Molecular evolution of GPCRs: CRH/CRH receptors. *J. Mol. Endocrinol.* **52**, T43-T60. doi:10.1530/JME-13-0238

Mankiewicz, J. L., Godwin, J., Holler, B. L., Turner, P. M., Murashige, R., Shamey, R., Daniels, H. V. and Borski, R. J. (2013). Masculinizing effect of background color and cortisol in a flatfish with environmental sex-determination. *Integr. Comp. Biol.* **53**, 755-765. doi:10.1093/icb/ict093

Mommsen, T., Vijayan, M. M. and Moon, T. (1999). Cortisol in teleosts: dynamics, mechanisms of action, and metabolic regulation. *Fish Physiol. Biochem.* **9**, 211-268.

Montero, D., Terova, G., Rimoldi, S., Tort, L., Negrin, D., Zamorano, M. J. and Izquierdo, M. (2015). Modulation of adrenocorticotrophin hormone (ACTH)-induced expression of stress-related genes by PUFA in inter-renal cells from European sea bass (*Dicentrarchus labrax*). *J. Nutr. Sci.* **4**, e16. doi:10.1017/jns.2015.6

Mork, L., Czerwinski, M. and Capel, B. (2014). Predetermination of sexual fate in a turtle with temperature-dependent sex determination. *Dev. Biol.* **386**, 264-271. doi:10.1016/j.ydbio.2013.11.026

Nakamura, M. (2009). Sex determination in amphibians. *Semin. Cell Dev. Biol.* **20**, 271-282. doi:10.1016/j.semcdb.2008.10.003

Nakamura, S., Watakabe, I., Nishimura, T., Toyoda, A., Taniguchi, Y. and Tanaka, M. (2012). Analysis of medaka sox9 orthologue reveals a conserved role in germ cell maintenance. *PLoS ONE* **7**, e29982. doi:10.1371/journal.pone.0029982

Nanda, I., Kondo, M., Hornung, U., Asakawa, S., Winkler, C., Shimizu, A., Shan, Z., Haaf, T., Shimizu, N., Shima, A. et al. (2002). A duplicated copy of DMRT1 in the sex-determining region of the Y chromosome of the medaka, *Oryzias latipes*. *Proc. Natl. Acad. Sci. USA* **99**, 11778-11783. doi:10.1073/pnas.182314699

Navarro-Martín, L., Viñas, J., Ribas, L., Díaz, N., Gutiérrez, A., Di Croce, L., Piferrer, F. and Whitelaw, E. (2011). DNA methylation of the gonadal aromatase (cyp19a) promoter is involved in temperature-dependent sex ratio shifts in the European sea bass. *PLoS Genet.* **7**, e1002447. doi:10.1371/journal.pgen.1002447

Nozu, R. and Nakamura, M. (2015). Cortisol administration induces sex change from ovary to testis in the protogynous wrasse, *Halichoeres trimaculatus*. *Sex. Dev.* **9**, 118-124. doi:10.1159/000373902

Ospina-Álvarez, N. and Piferrer, F. (2008). Temperature-dependent sex determination in fish revisited: prevalence, a single sex ratio response pattern, and possible effects of climate change. *PLoS ONE* **3**, e2837. doi:10.1371/journal.pone.0002837

Ota, S., Hisano, Y., Muraki, M., Hoshijima, K., Dahlem, T. J., Grunwald, D. J., Okada, Y. and Kawahara, A. (2013). Efficient identification of TALEN-mediated genome modifications using heteroduplex mobility assays. *Genes Cells* **18**, 450-458. doi:10.1111/gtc.12050

Pfaffl, M. W., Horgan, G. W. and Dempfle, L. (2002). Relative expression software tool (REST©) for group-wise comparison and statistical analysis of relative expression results in real-time PCR. *Nuceic Acids Res.* **30**, e36. doi:10.1093/nar/30.9.e36

Ribas, L., Liew, W. C., Díaz, N., Sreenivasan, R., Orbán, L. and Piferrer, F. (2017). Heat-induced masculinization in domesticated zebrafish is family-specific and yields a set of different gonadal transcriptomes. *Proc. Natl. Acad. Sci. USA* **114**, E941-EE50. doi:10.1073/pnas.1609411114

Saito, D., Morinaga, C., Aoki, Y., Nakamura, S., Mitani, H., Furutani-Seiki, M., Kondoh, H. and Tanaka, M. (2007). Proliferation of germ cells during gonadal sex differentiation in medaka: insights from germ cell-depleted mutant *zenzai*. *Dev. Biol.* **310**, 280-290. doi:10.1016/j.ydbio.2007.07.039

Shibata, Y., Paul-Prasanth, B., Suzuki, A., Usami, T., Nakamoto, M., Matsuda, M. and Nagahama, Y. (2010). Expression of gonadal soma derived factor (Gsdf) is spatially and temporally correlated with early testicular differentiation in medaka. *Gene Expr. Patterns* **10**, 283-289. doi:10.1016/j.gep.2010.06.005

Smith, G. W., Aubry, J.-M., Dellu, F., Contarino, A., Bilezikjian, L. M., Gold, L. H., Chen, R., Marchuk, Y., Hauser, C., Bentley, C. A. et al. (1998). Corticotropin releasing factor receptor 1-deficient mice display decreased anxiety, impaired stress response, and aberrant neuroendocrine development. *Neuron* **20**, 1093-1102. doi:10.1016/S0896-6273(00)80491-2

Stemmer, M., Thumberger, T., del Sol Keyer, M., Wittbrodt, J. and Mateo, J. L. (2015). CCTop: an intuitive, flexible and reliable CRISPR/Cas9 target prediction tool. *PLoS ONE* **10**, e0124633. doi:10.1371/journal.pone.0124633

Sztainberg, Y. and Chen, A. (2012). Neuropeptide regulation of stress-induced behavior: insights from the CRF/urocortin family. In *Handbook of Neuroendocrinology* (ed. D. W. Pfaff and J. E. Levine), pp. 355-375. San Diego: Academic Press.

Timpl, P., Spanagel, R., Sillaber, I., Kresse, A., Reul, J. M. H. M., Stalla, G. K., Blanquet, V., Steckler, T., Holsboer, F. and Wurst, W. (1998). Impaired stress response and reduced anxiety in mice lacking a functional corticotropin-releasing hormone receptor 1. *Nat. Genet.* **19**, 162-166. doi:10.1038/520

Trayer, V., Hwang, P.-P., Prunet, P. and Thermes, V. (2013). Assessment of the role of cortisol and corticosteroid receptors in epidermal ionocyte development in the medaka (*Oryzias latipes*) embryos. *Gen. Comp. Endocrinol.* **194**, 152-161. doi:10.1016/j.ygcen.2013.09.011

Tsalafouta, A., Papandroulakis, N., Gorissen, M., Katharios, P., Flik, G. and Pavlidis, M. (2014). Ontogenesis of the HPI axis and molecular regulation of the cortisol stress response during early development in *Dicentrarchus labrax*. *Sci. Rep.* **4**, 5525. doi:10.1038/srep05525

Vaughan, J., Donaldson, C., Bittencourt, J., Perrin, M. H., Lewis, K., Sutton, S., Chan, R., Turnbull, A. V., Lovejoy, D., Rivier, C. et al. (1995). Urocortin, a mammalian neuropeptide related to fish urotensin I and to corticotropin-releasing factor. *Nature.* **378**, 287-292. doi:10.1038/378287a0

Wendelaar Bonga, S. E. (1997). The stress response in fish. *Physiol. Rev.* **77**, 591-625. doi:10.1152/physrev.1997.77.3.591

Yamaguchi, T. and Kitano, T. (2012). High temperature induces cyp26b1 mRNA expression and delays meiotic initiation of germ cells by increasing cortisol levels during gonadal sex differentiation in Japanese flounder. *Biochem. Biophys. Res. Commun.* **419**, 287-292. doi:10.1016/j.bbrc.2012.02.012

Yamaguchi, T., Yoshinaga, N., Yazawa, T., Gen, K. and Kitano, T. (2010). Cortisol is involved in temperature-dependent sex determination in the Japanese flounder. *Endocrinology.* **151**, 3900-3908. doi:10.1210/en.2010-0228

Yamamoto, Y., Hattori, R. S., Kitahara, A., Kimura, H., Yamashita, M. and Strüssmann, C. A. (2013). Thermal and endocrine regulation of gonadal apoptosis during sex differentiation in pejerrey *Odontesthes bonariensis*. *Sex. Dev.* **7**, 316-324. doi:10.1159/000353506

Yatsu, R., Miyagawa, S., Kohno, S., Saito, S., Lowers, R. H., Ogino, Y., Fukuta, N., Katsu, Y., Ohta, Y., Tominaga, M. et al. (2015). TRPV4 associates environmental temperature and sex determination in the *American alligator*. *Sci. Rep.* **5**, 18581. doi:10.1038/srep18581

Zhang, Z. and Hu, J. (2007). Development and validation of endogenous reference genes for expression profiling of medaka (*Oryzias latipes*) exposed to endocrine disrupting chemicals by quantitative Real-Time RT-PCR. *Toxicol. Sci.* **95**, 356-368. doi:10.1093/toxsci/kfl161

Zhang, X., Guan, G., Li, M., Zhu, F., Liu, Q., Naruse, K., Herpin, A., Nagahama, Y., Li, J. and Hong, Y. (2016). Autosomal gsdf acts as a male sex initiator in the fish medaka. *Sci. Rep.* **6**, 19738. doi:10.1038/srep19738

Zhou, L., Charkraborty, T., Zhou, Q., Mohapatra, S., Nagahama, Y. and Zhang, Y. (2016). Rspo1-activated signalling molecules are sufficient to induce ovarian differentiation in XY medaka (*Oryzias latipes*). *Sci. Rep.* **6**, 19543. doi:10.1038/srep19543

Supplementary information

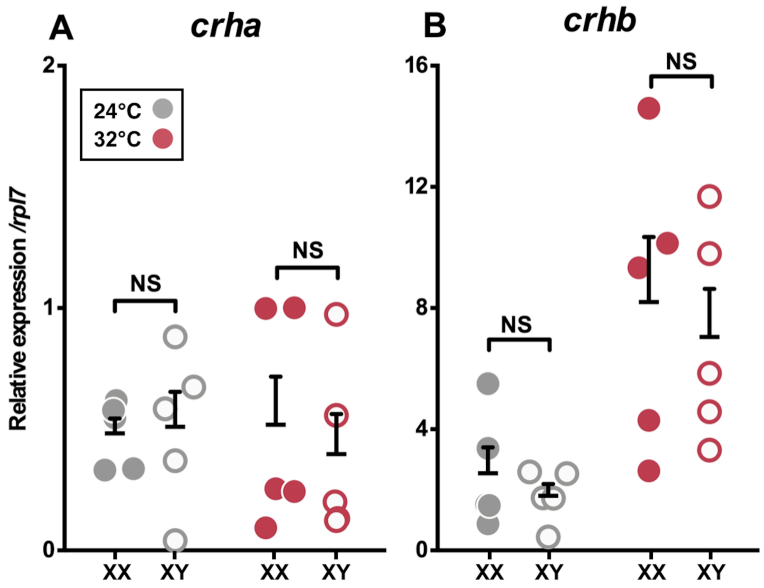

Fig. S1. Gene expression profiles of *crha* **(A)** and *crhb* **(B)** in embryos reared at 24 °C (grey circles) and 32 °C (orange circle). These data were measured by qPCR analysis in whole embryos at stage 37. Gene expression levels are expressed relative to the XX 24 °C treatment. Quantification method was performed using the $2^{-\Delta\Delta Ct}$ method and values were normalized by the respective values of *rpl7*. Genotypic sex was determined at stages 33 and 37 by the presence/absence of the *dmy* gene; XX and XY are represented by filled circles and open circles, respectively. Horizontal bars indicate mean, with its respective standard error of the mean. The *p* values are indicated when transcript abundance between temperature treatments at the same developmental stage differ statistically (REST©; $p < 0.05$).

Development • Supplementary information

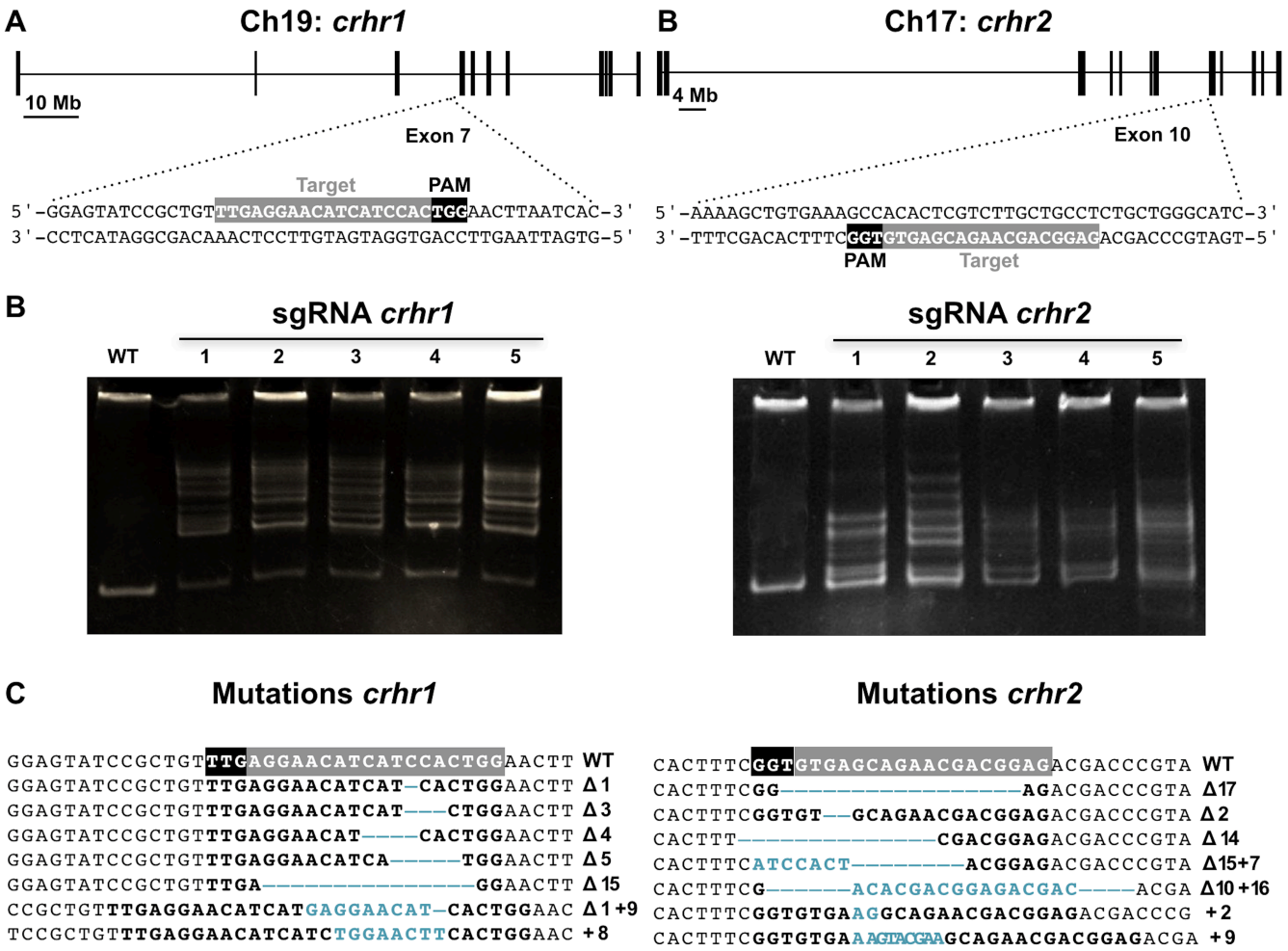

Fig. S2. Schematic representation of the genomic structure of *crhr1* and *crhr2* **(A)**. Coding exon regions are shown as solid boxes. The targeting sequence of sgRNA for each gene is indicated by a gray box, adjacent to NGG protospacer adjacent motif (PAM) sequence in black box. **(B)** Multiple heteroduplex bands were shown in PCR amplicons from each sgRNA of receptors injected embryo, wild type (WT) embryo a single band was shown. **(C)** Subcloned sequences observed in the *cas9* (wt), *cas9*+sgRNA*crhr1* embryos, and the *cas9*+sgRNA*crhr2* embryos at F1. Blue dashes and letters indicate the identified mutations. The size of indels is shown to the right of each mutated sequence. Numbers on the right edge indicate the numbers of mutated clones identified from all analyzed clones from each embryo.

Development • Supplementary information

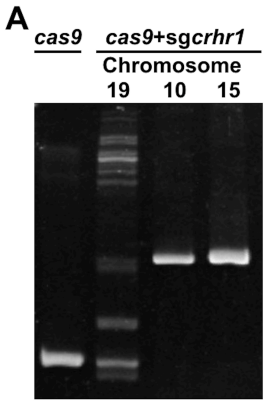

sgRNA	Site No.	Sequence	% Mutation
crhr1	Target Ch 19	TTGAGGAACATCATCCACTGG	96,6% (29/30)
	Off Target Ch 10	GTGAGTAACATCATCCACAGG	0% (0/5)
	Off Target Ch 15	TTGAGGACCATCATCCTCAGG	0% (0/5)

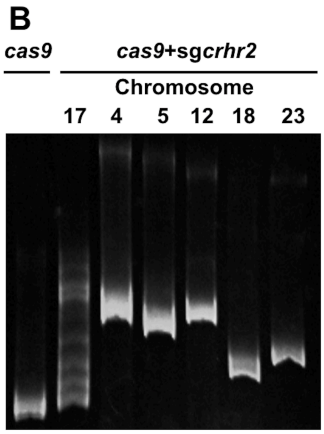

sgRNA	Site No.	Sequence	% Mutation
crhr2	Target Ch 17	GAGGCAGCAAGACGAGTGTGG	100% (30/30)
	Off Target Ch 4	GAGTCAGGAAGACGAGTGAGG	0% (0/5)
	Off Target Ch 5	AAGGCAGCAACACGAGTGAGG	0% (0/5)
	Off Target Ch 12	GATGCAGCAAGACGAGAGCGG	0% (0/5)
	Off Target Ch 18	GAGGCAGCAAGACAAGGGGGG	0% (0/5)
	Off Target Ch 23	GAGGCAGCAACACCAGTGCGG	0% (0/5)

Fig. S3. Images of heteroduplex mobility assay (HMA) for detecting off-target alterations. Potential off-target loci for **(A)** *crhr1* (1.1.2 sgRNA), or **(B)** *crhr2* (2.2.2 sgRNA) were analyzed using genomic DNA extracted from five embryos coinjected with 100 ng/mL of *cas9* mRNA and either 25 ng/mL of sgRNA. Tables indicate the target and potential off-target loci identified with respective chromosome (Ch), sequence,percentage of biallelic mutation detected and number of embryos with biallelic mutations/total of eggs injected are shown in parentheses. Sequences of the off-target primers used for HMA were listed in **Tables S1**.

Development • Supplementary information

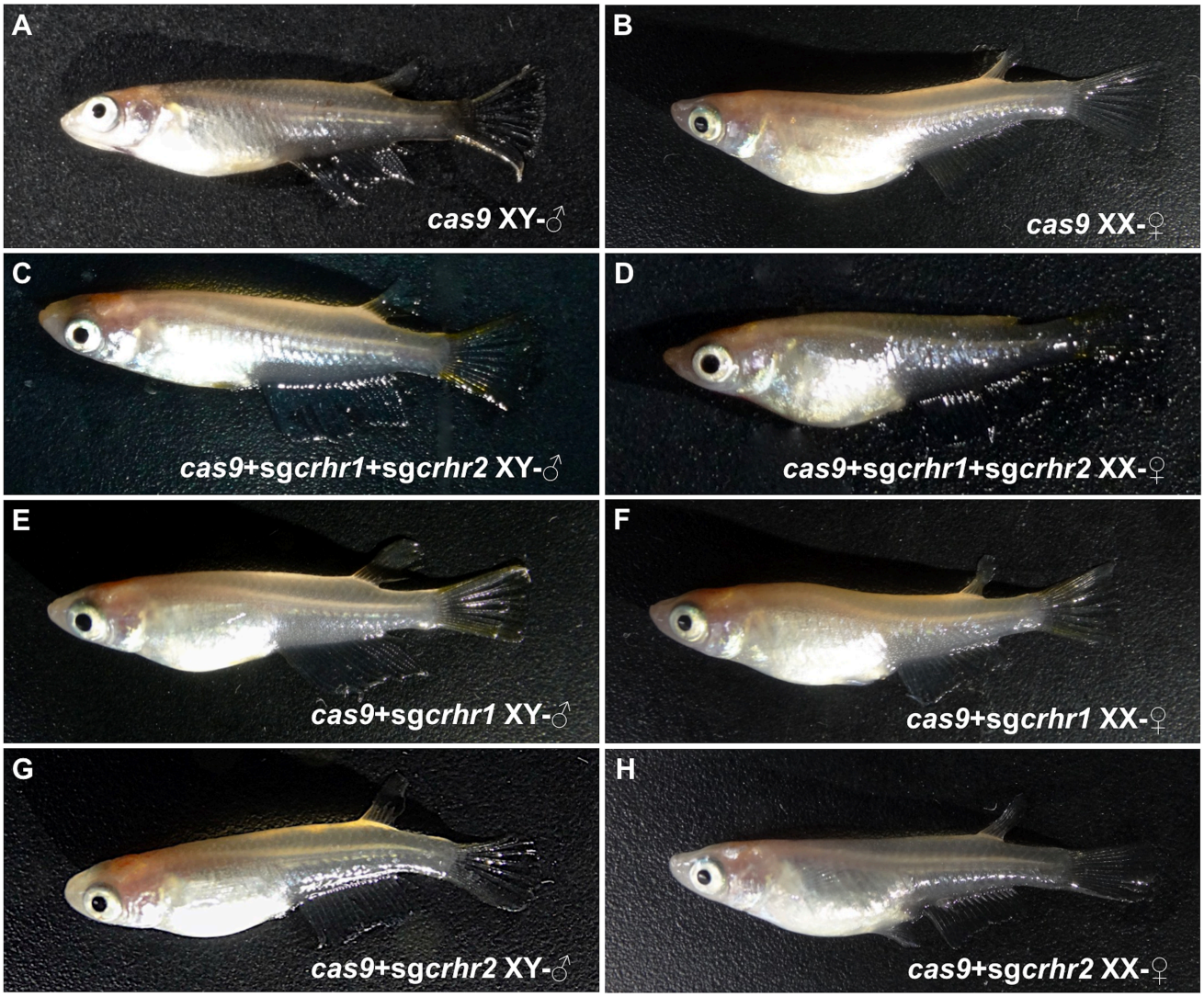

Fig. S4. The medaka biallelic mutants did not exhibit external morphological differences with the wild-type (*cas9*). Adults medaka fish derived from embryos injected with *cas9* **(A, B)**, *cas9*+sgRNA-*crhr1* **(B, C)**, *cas9*+sgRNA-*crhr2* **(D, E)**, and *cas9*+sgRNA-*crhr1*+-*crhr2*, were reared at 26 °C (CT) until 60 dph.

Development • Supplementary information

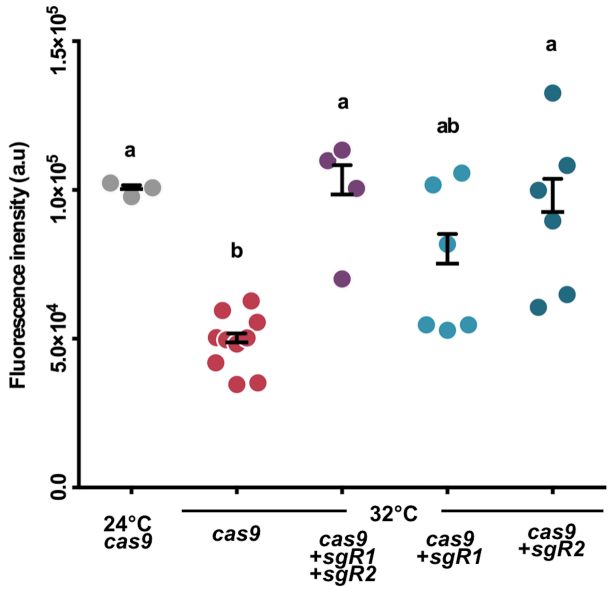

Fig. S5: Fluorescence intensity expressed in arbitrary units (a.u) per square micrometer of immunoreactive Acth cells in embryos injected with *cas9* (controls at 24 °C and 32 °C), *cas9*+sgRNA-*crhr1, cas9*+sgRNA-*crhr2* and both *cas9*+*crh* receptors at 32 °C. Horizontal bars indicate mean, with its respective standard error of the mean. Different letters indicate statistically significant differences between treatments (one-way ANOVA, followed by a Tukey's multiple comparison test; $p < 0.05$).

Development • Supplementary information

Table S1. Primer Sequences.

Gene	Primer sequence	Accession Number	Reference
RT-qPCR			
crha	Fw. 5′-GCTGTCCTTGTAAAGTTTTTGGG-3′ Rv. 5′-AGCGGTTTGGTTCGTCTTAG-3′	ENSORLG00000006816	
crhb	Fw. 5′-CTGCTTGTTGCCTTTTTGCC-3′ Rv. 5′-GAATGGGACTAGACTGTTGCTG-3′	ENSORLG00000008503	
uts1	Fw. 5′-AACCACAGTGGAATCCGAAC-3′ Rv. 5′-GATGCCTCCATTGTTTGGTC-3′	LC176788	
ucn2	Fw. 5′-AGCTTAGAGCCGTTTTGTGC-3′ Rv. 5′-TGCGGAGTTCAGTGTTTCAC-3′	LC176789	
ucn3	Fw. 5′-CCAACATCATGAACGTCCTC-3′ Rv. 5′-AAATGTAGTGCGCCGAGAAG-3′	LC176790	
crhr1	FW. 5′-AATTGACCATGAGCCCTGA-3′ RV. 5′-GATGTTTGGAGAAGGCTGCT-3′	ENSORLG00000012904	
crhr2	FW. 5′-TTGCTTCAGCTGATTGACCAC-3′ RV. 5′-GCATCCTTCAACGAACATCC-3′	ENSORLG00000017621	
acth	FW. 5′-TCAAACCAAACGCTCCTACTCC-3′ RV. 5′-TCCTCATCTCACCTGGGAAAAC-3′	ENSORLG00000001386	
gsdf	FW 5′-GGGCTGGACACTATTCGAGA-3′ RV 5′-CATGACACAGAGGAGCTGGA-3′	ENSORLG00000006451	Zhou et al. 2016
sox9a2	Fw. 5′-CTCCGACGCTCCCAGTCCCA-3′ Rv. 5′-GACGGCCGGGTGTTTTCGGT-3	ENSORLG00000007960	Zhou et al. 2016
cyp19a1a	Fw. 5′-AGCTTATTTTTGCCCAAGGCC-3′ Rv. 5′-TTGAGCAGCAGGAGCATGAAA-3	ENSORLG00000002949	Zhou et al. 2016
cyp11b	Fw. 5′-CAGGTTATACCCAGTAGGAATC-3′ Rv. 5′-GTCTTAGGTTGCAGGATCAG-3	ENSORLG00000010480	Kurokawa et al., 2007.
hsd11b2	Fw. 5′ -GAACAACGCTGGTGTTTGTG-3′ Rv. 5′ –AAGTTGACCTCCATGCATCC-3′	ENSORLG00000000323	
rpl7	FW 5′-CGCCAGATCTTCAACGGTGTAT-3′ RV 5′-AGGCTCAGCAATCCTCAGCAT-3′	DQ118296	Zhang and Hu et al. 2007
PCR sexing			
dmy	FW 5′-CAACTTTGTCCAAACTCTGA-3′ RV 5′-TGATGCAGCATTTTGACACATTTA-3′	ENSORLG00000020486	Nanda et al., 2002)
β-actin	FW 5′-GGATGACATGGAGAAGATCTGG-3′ RV 5′-ATGGTGATGACCTGTCCGTC-3′	ENSORLG00000013676	
Heteroduplex mobility assay (HMA)			
crhr1	FW 5′-TCCTTAGTGCCGCATCT AC-3′ RV 5′-AGTTACCACGCACCACGTTG-3′	ENSORLG00000012904	
crhr2	FW 5′-AGAAACTTGGCTTGCTGATG-3′ RV 5′-TGTTTAACAGCTCTCTGCAG-3′	ENSORLG00000017621	
Off-target HMA			
Chr10	FW 5′-GGGCGCTTTCCTACACCAG-3′ RV 5′-TCACACATAAAGGGCCGCAG-3′	ENSORLG00000001972	

Development • Supplementary information

Table S1. Primer Sequences.

Chr15	FW 5′-TCGTGGGGAAGCTCATGTTC-3′ RV 5′-CCGGTTCAGATGACCCAACA-3′	ENSORLG00000000740	
Chr4	FW 5′-AGGGATGGGACACGTCATAG-3′ RV 5′-TTATGCTGCTCAATCGTCCTC-3′	Chr4: 31,779,474-31,779,496	
Chr5	FW 5′-CCATGCCAGTCCAATCCTGG-3′ RV 5′-TCAGAGGAAGGCCTGTGTTC-3′	Chr5: 790,585-790,607	
Chr12	FW 5′-CTTTAGTGTGCCAGAAGTGAT-3′ RV 5′-TTCCTGTTACTCCCAACCTG-3′	Chr12: 3,702,673-3,745,116	
Chr18	FW 5′-ACATCTCACCCGCTAGTATC-3′ RV 5′-TGAACCACATTCTCGTGGTC-3′	Chr18: 729,045-775,628	
Chr23	FW 5′-TCAGCGTAGCAACCACAGAG-3′ RV 5′-GTTGGAGCCAGGTGTCCATG-3′	ENSORLG00000008900	

Table S1. Primers sequences used in the present study. The NCBI accession numbers and the respective references were added to each gene.

Development • Supplementary information